Journal of Physics: Conference Series **114** (2008) 012011 doi:10.1088/1742-6596/114/1/012011

A Road Map to Extreme High Vacuum

Philip Adderley, Ganapati Myneni

Jefferson Lab
12000 Jefferson Ave, Newport News, VA; 23606

adderley@jlab.org, rao@jlab.org

Abstract. Ultimate pressure of a well-designed vacuum system very much depends on pretreatments, processing and procedures [1, 2]. Until now much attention has been paid to minimizing hydrogen outgassing from the vacuum chamber wall materials, however, procedures and processing deserve further scrutiny. For reducing the gas load, high sensitivity helium leak detection techniques with sensitivities better than 1×10^{-12} Torr l/sec should be used. Effects that are induced by vacuum instrumentation need to be reduced in order to obtain accurate pressure measurements. This paper presents the current status of the CEBAF DC photogun. This state of the art technology is driving the need for Extreme High Vacuum (XHV). We also present sensitive helium leak detection techniques with RGA's, vacuum gauge and RGA calibration procedures, metal sponges for cryosorption pumping of hydrogen to XHV, low cost surface diffusion barriers for reducing the hydrogen gas load and clean assembly procedures. Further, alternative backing pump systems based on active NEGs [3] for turbo molecular pumps are also discussed.

1. Introduction

At Jefferson Lab, the Continuous Electron Beam Accelerator Facility (CEBAF) was built to study the hadronic structure of the nucleus using polarized electrons. The generation of polarized electrons, via laser stimulated photoemission from a GaAs photocathode held at -100 keV in an ultra-high vacuum system is known as the photogun. The photocathode lifetime is limited by the vacuum conditions, with residual gas ionization and ion-back-bombardment limiting operational lifetime.The need for improved lifetime is the motivation toward achieving XHV conditions of pressures lower than 7.5×10^{-13} Torr.

2. Polarized Electron Guns – Vacuum Requirements and Status

The CEBAF photoguns have evolved over time from the first generation gun comprised of a single stainless steel (SS) chamber with photocathode surface-chemical preparation occurring in the same chamber, and pumped by a diode ion pump. Short photocathode lifetimes drove design changes toward the second generation photogun by adding a SS NEG chamber, with the chemical preparation of the photocathode surface occurring in the original SS main chamber, and pumped with the diode ion pump. Replacement of the photocathode with these photogun designs required venting the system to atmosphere with dry nitrogen, and rebaking at 250°C for 30 hours. This past summer, the "vent&bake" a CEBAF photogun was replaced with an improved third generation NEG load-locked photogun system and it is shown schematically in Figure 1. This gun again uses combined NEG and ion pumping, but the photocathode chemical preparation chamber is now separate from the high voltage NEG chamber where the vacuum requirements are most stringent. In addition, the load-locked

gun design allows photocathode material to be changed without venting the high voltage chamber to atmosphere and thus alleviates a re-bake of the entire system.

Improvements to the vacuum system of the load-locked gun were implemented to reduce the ultimate pressure in the high voltage chamber. The main NEG chamber was vacuum fired at 950ºC for four hours prior to welding the end conflat flanges and was coated with a homemade NEG film on the interior surfaces (Ti/Zr/V). Measurement of the ultimate pressure in this system compared to the "vent&bake" photoguns, as shown in Figure 3, indicated a slight improvement in the ultimate pressure, as measured with an extractor gauge.

For the "vent&bake" photogun, Figure 2 and Figure 3 show the results of an RGA vs extractor gauge measurement with good agreement on the ultimate pressure. The extractor gauge and the RGA used for these measurements were cross calibrated on a conventional gauge calibration system as well as with saturated hydrogen vapor pressure at 4.25 K and low pressure helium environments at cryogenic temperatures; the details of which are provided in a later section of this paper.

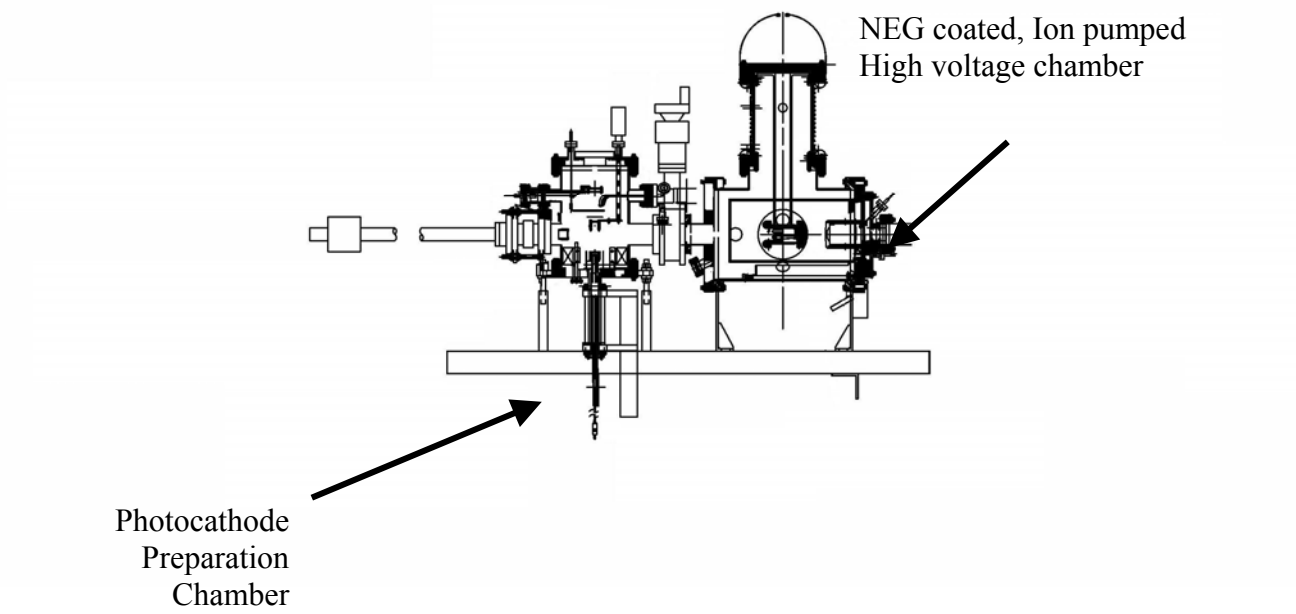

Figure 1: CEBAF load-lock photoelectron gun. Chemical preparation of the photocathode takes place in the preparation chamber, separating chemical processing from the best vacuum in the high voltage chamber. The load-locked system also allows introduction of new photocathode material without venting and re-baking the entire system.

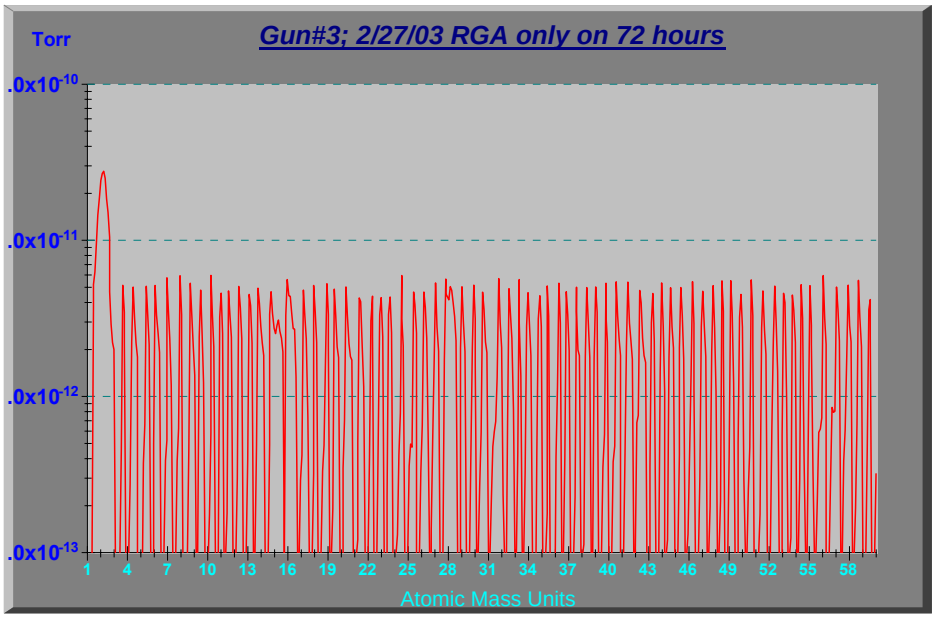

Figure 2: Residual Gas Analyzer trace for the "vent&bake" photogun. Hydrogen partial pressure dominates in UHV systems, and ultimate pressure is less than 2.5×10^{-11} Torr with correction for hydrogen high throughput in the analyzer by dividing the pp of H_2 by 1.5 [4]

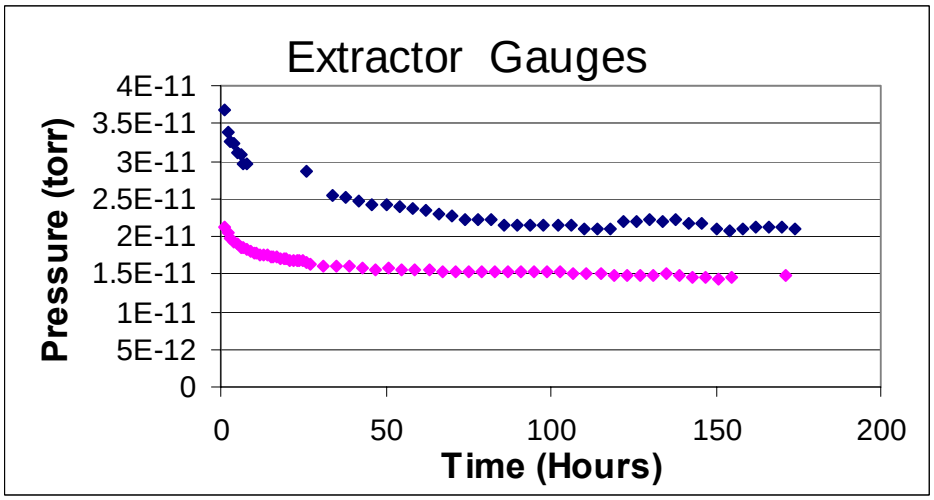

Figure 3: Extractor gauge readings as a function of time for two "vent&bake" CEBAF photoguns. Both show that at least 50 hours are necessary before stabilization of extractor gauge readings, and both in relatively good agreement with partial pressure measurement of hydrogen made with an RGA as shown in Figure 2. Extractor gauge readings are corrected (multiplied by a factor of 2.7) to reflect that the gauge is calibrated for nitrogen and the predominant gas in this system is hydrogen.

2.1 Virtual - Real Leaks, Outgassing and Ultimate Pressure

Many details must be considered and understood before an ultra-high vacuum system can be pushed into the extreme high vacuum range. Studying equation 1 for the effective pump speed [5] will help us understand the complexity of the problems we need to solve for obtaining the best possible ultimate high vacuum.

$$S_{effective} = \left(Q_{surfaces} A + Q_{real} + Q_{virtual}\right) / P_{ultimate} \qquad (1)$$

Where $S_{effective}$ is the effective pump speed, $Q_{surface}$ is the outgassing rate from the internal vacuum surfaces, A is the total surface area, Q_{real} is the outgassing contributions from real leaks, $Q_{virgual}$ is the outgassing contributions from virtual leaks, and $P_{ultimate}$ is the ultimate pressure of the system.

The outgassing terms are significant in that they contain contributions from various sources namely, wall outgassing of the chamber walls plus all other surfaces inside the vacuum. The chamber walls have the condition of atmosphere on one side and vacuum on the other side, and tend to have a different outgassing rate than the surfaces completely inside the vacuum chamber. Well characterized materials with pre-processing, as well as the use of internal or external barrier coatings including NEG coatings, are used to limit chamber wall outgassing and show promising results in achieving lower pressures (as presented later in this paper).

Virtual leaks, which are hard to identify and eliminate, are comprised of captured volumes within the vacuum system. They include blocked holes and screw threads in the vacuum. Of note: the vented screw design allow evacuation of trapped gases in the bottom of a blind tapped hole, but does not afford complete evacuation of the trapped gases in the threads themselves which trap gasses between their major and minor diameters. The best evacuation scenario for screw threads is having a channel cut across the threads to allow each thread circumference of the screw to be vented completely along the length of the screw as well as the bottom of the tapped hole.

Real external leaks may also exist, and most likely will be those that are smaller than the detectable level provided through the standard leak checking method. Leak checking at the lowest possible levels, at or below the target pressure for XHV, is necessary to eliminate tiny leaks before and after a bake. RGA's are extremely sensitive to contamination and outgassing of their internal components, therefore the degas cycle must be used to fully degas the instrument. The RGA's history, indicative of where it was used before, is also a factor requiring attention. Baring these factors, the only limitation then, for small leak detection, is the ultimate acheivable pressure in the system after a bake, using a contaminant free RGA.

2.1.1 Sensitive Helium Leak Detection with RGA

Helium is a stable gas and its partial pressure contribution in a vacuum system is real. For very sensitive leak checking and certification of leak levels, the use of a calibrated helium leak, at the target ultimate pressure of the system, will afford discerning small leaks with quantifiable accuracy and is shown in Figure 4.

The real leak rate of the system can be calculated with the help of the equation

$$Q_L = \frac{P_L - P_0}{P_S - P_0} \cdot Q_S \qquad (2)$$

where Q_L= Leak Rate; P_L = Leak He partial pressure; P_0 = Background He partial pressure, P_s = 'Standard He Leak' partial pressure, Q_s = 'Standard He leak' leak rate

It is clear that with a background helium partial pressure in the 10^{-13} Torr range, with less than 1 l/s pumping speed for He in the ion NEG pumped system and by checking the sensitivity of the RGA with a calibrated Helium leak rate Q_S of 1×10^{-10} Torr ls^{-1}, one can discern leaks smaller than $1x10^{-12}$ Torr ls^{-1}level with ease.

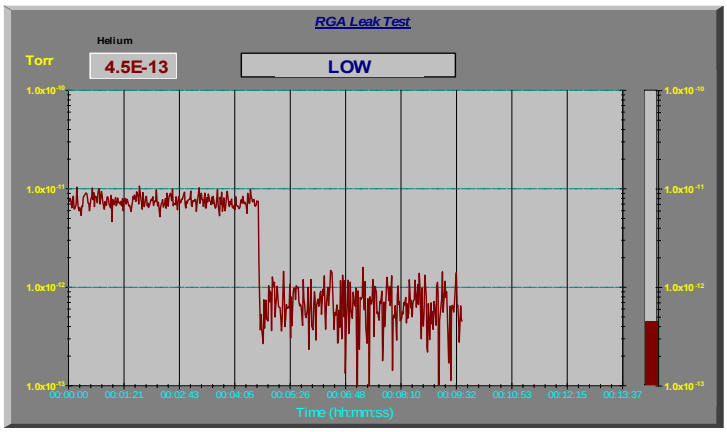

Figure 4: Residual gas analyzer trace during leak checking with the calibrated leak first open then closed. With this known calibrated leak, the magnitude of any leaks detected in the experimental system can be quantified.

2.1.2 Outgassing

The rate of rise, or the accumulation method, was used for making the outgassing rate measurements reported here [6]. The outgassing rates for three vacuum chambers were measured with the spinning rotor gauge and are shown in Figure 5 as a function of bake number. Two of the chambers were from a standard "vent&bake" CEBAF gun configuration, constructed of 304 stainless steel. The first was untreated, while the second was vacuum fired at 950ºC for four hours before the conflat flanges were welded on. The third chamber was a larger gun chamber for the free electron laser machine at Jefferson Lab (FEL), made from 316LN stainless steel. It was heat processed after initial assembly by baking with air outside and vacuum inside at 400ºC for 11 days. This heat-treating process afforded the best outgassing rate of all.

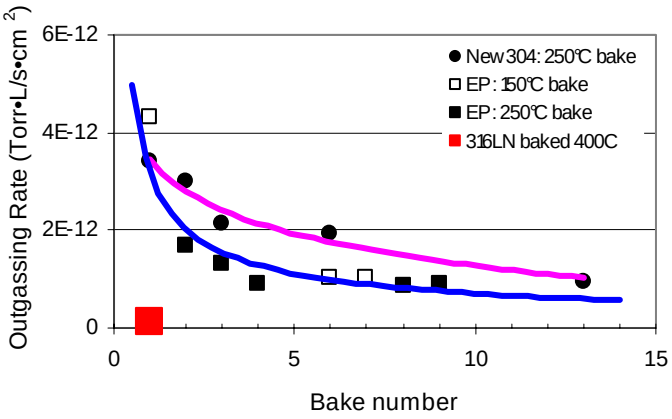

Figure 5: Outgassing rates for 304 stainless steel chambers following sequential bakes.

The top curve shows the data for untreated 304 SS, while the bottom curve shows improvements achieved through vacuum firing at 950ºC for four hours. The data point on the x-axis shows the outgassing rate for the heat treated 316LN chamber at 400ºC. The outgassing rate measurement for this system was performed without venting the system to atmosphere between the heat treatment and

the measurement, so the posted outgassing rate is the best possible for this process. An effective outgassing rate may be different, when measured after venting a system and re-baking it at 250ºC.

2.1.3 Ultimate Pressure and Measured Pumping Speed

The ultimate pressure in various photogun chambers was calculated using the measured outgassing rate of $1x10^{-12}$ TorrL/scm^2 for SS and the manufacturer's quoted pump speeds for the NEG pumps. Figure 6 shows the measured and calculated ultimate pressures for various test chambers containing different NEG getter surfaces. The calculated ultimate pressures in all the chambers are significantly lower than the measured pressures. The right-most data point is for the load-lock photogun.

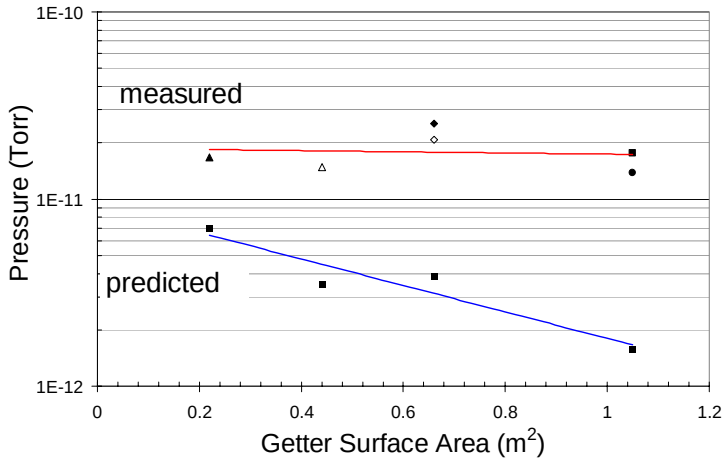

Figure 6: Measured vs. predicted pressure in various photoguns and test chambers

The ion pump's pumping speed was not included in the calculation, however, since the pumping speed of the ion pump for hydrogen is negligible in comparison to the pumping speed of the NEG strips, this does not account for the pressure discrepancies. The ion pump is expected to help reduce the pressure by pumping the inert gasses and methane, which the NEGs do not adequately pump. Explanations for this discrepancy between the estimated and measured pressures are unclear. Perhaps the measurement accuracy of the gauges is affected by contamination of the chambers leading to oxides of carbon and methane, which in turn can affect gauge readings.

The inside surface of the main high voltage chamber of the load-lock gun was coated with titanium, vanadium and zirconium based on the Benvenuti sputtering recipe [7]. The coating was analyzed using electron desorption spectroscopy and found to have a composition of 25, 50, 25% (for Ti,V, Zr) and a total pumping speed of ~200 l/s (0.02 l/scms^2). The composition is similar to SAES' commercial ST707 getters.

Pumping speed measurements were conducted using the orifice method [8]. RGAs monitor the partial pressure of hydrogen on either side of an orifice. Knowing the conductance of the orifice and the pressure drop across the orifice, one can determine the pumping speed of the NEGs inside the test chamber. The measured pumping speed for SAES getter modules and the TiVZr coatings are shown in Table **1**. It is clear from this data that the SAES ST707 getter modules need to be activated by direct heating to ~400 ºC for `1 hour for full activation. However, our preferred activation is during the bake out of the chambers at 250 ºC for 30 hours, and the getters do not get fully activated (~60%), and thus show a lower pumping speed.

Pump style	**Speed for p>8x10^{-11} Torr**	
	Bake only	Resistive activation
SAES ST707	450 l/s for WP950 module	1150 l/s
Ti/Zr/V coating	0.02 l/s.cm^2 for 200 l/s total	

Table 1: Pump speeds for commercial getter modules and Ti/Zr/V coatings applied at Jefferson Lab.

2.2 Photocathode Lifetime

A measurement of the photocathode lifetime in two different load lock gun designs is shown in Figure 7. An improvement in lifetime by a factor of ~ 2 for bulk GaAs in the latest gun design over its predecessor prototype (referred to as BP in Figure 7) without the NEG coated high voltage chamber. Interestingly, the ultimate pressure readings for both guns were essentially identical [9]. Therefore, the need for direct gun comparisons, gauge calibration for determining its sensitivity and paying attention to its application history and orientation will ensure proper ultimate pressure measurements and further understanding of the photoguns operation.

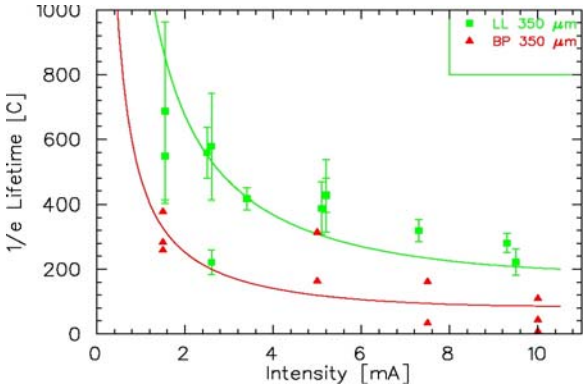

Figure 7: Lifetime measurement for the two load-locked photoguns. The initial Prototype load-locked gun, bottom trace "BP", shows lifetimes at all currents a factor of ~ 2 lower than the newer load-locked electron gun which incorporated a vacuum fired, Ti/Zr/V getter coated high voltage chamber, and fully activated NEG modules.

3. Vacuum Gauge and RGA Conventional Calibrations

The calibration chamber shown in Figure 8 is designed with symetrical ports for adding several Ionization Gauges, RGAs, and a spinning Rotor Gauge (SRG). It is pumped by a Pfeiffer TSU180H Turbo, which has a relatively high hydrogen compression ratio. The gas inlet system has a fine flow-controlling valve for each gas type for introduction into the main chamber. The cleanliness with which the chamber and its components were handled and fabricated is evident in the RGA scans (Figure 8a). The pressure reached within 26 hours punctuates that an 8x10^{-10} Torr pressure is a very good vacuum

for an unbaked Turbo system. This condition indicates that one can achieve low ultra high (UHV) vacuum pressures without baking provided contaminants are eliminated from the system. After baking the system at 150ºC for 24 hours, the ultimate pressure is measured at $4x10^{-11}$ Torr with gauge corrections for hydrogen. There is good agreement between the calculated pressure for the system using the manufacturer's specifications for the Turbo's hydrogen pumping speed and the RGA partial pressure of hydrogen compared with the extractor gauge (raw reading ~ $1.5x10^{-11}$ Torr). The system has a wide calibration pressure range for gauges, which is $1x10^{-2}$ – $5x10^{-11}$ Torr and was effectively used for a large number of investigations [10-14]. Several commercial standard gauges were incorporated in this system to facilitate this wide calibration range: including an MKS Baratron, an SRG (spinning Rotor Gauge), an Extractor and an SRS RGA. Later, an Axtran gauge was added. Both the RGA and extractor gauges were calibrated with this system using the SRG as the low pressure standard. The RGA and a set of extractor gauges were further cross-compared with the cryogenic calibration systems as discussed in the following section.

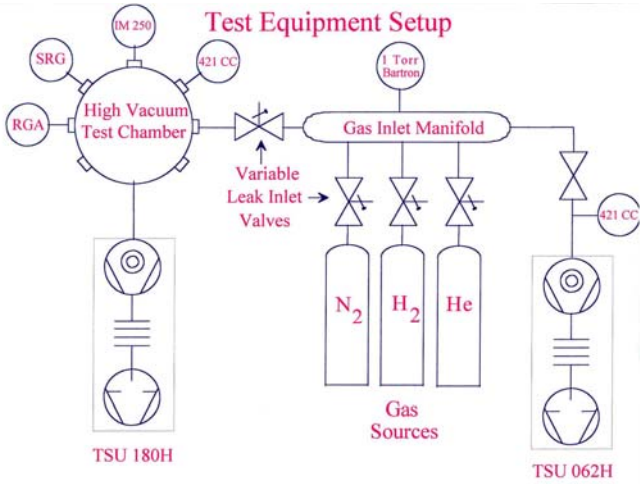

Figure 8: Calibration test stand for cross comparison of gauges.

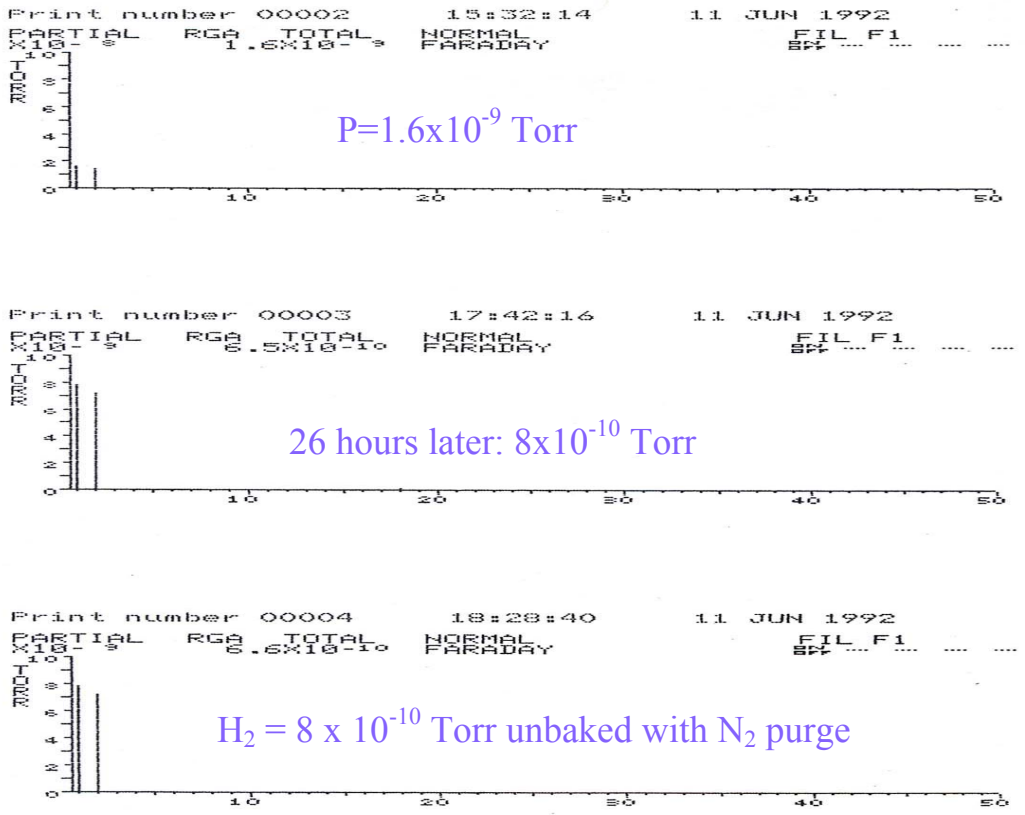

Figure 8(a): Calibration test stand RGA traces.

3.1 Gauge Calibrations Based on Fundamental Physics Principles

Jefferson Lab has a wealth of liquid helium cryogenic systems which afford novel low pressure calibration setups with residual helium and the saturated vapor pressure of hydrogen. Cryopumping, thus, offers very low pressures which can be estimated from first principles of physics. We have used saturated hydrogen vapor pressure and the residual helium pressures for cross comparison of an RGA with both a cold and room temperature extractor gauge.

The extractor gauge that is to be calibrated is installed in a vacuum vessel and submerged in a cryostat as shown in the Figure 9. In this set up we used He residual gas pressure for cross comparison of the earlier calibrated RGA and extractor gauges at pressures below 1×10^{-9} Torr which was the lowest pressure below which NIST does not offer gauge calibrations. The extractor gauge readings and its sensitivity are based on the gas density and temperature. Since the extractor gauge controller assumes that the gauge is operating at room temperature, a temperature correction has to be applied by multiplying the gauge readings with 4.25/294 for direct comparison with the RGA which is at room temperature. The RGA helium partial pressure readings are corrected for thermal transpiration. As the temperature of the cryostat is raised, from 4.5K to 10.5K, helium desorbs from the walls at 10.5K. Above 12K the extractor gauge reading increases due to hydrogen desorption from the vacuum system walls. Data in Figure 9 show that the RGA and the extractor gauge readings track quite well until 15 K. The cold extractor gauge shows a small amount of hydrogen desorbing until 20 K above which hydrogen desorption accelerates significantly causing disagreement with the RGA which is monitoring just the partial pressure of helium. At the lowest pressures there is a disagreement between RGA and extractor gauge readings. This is reasonable because the extractor gauge reading includes the partial pressure of hydrogen while the RGA is only monitoring the helium partial

pressure. However, when the extractor gauge was shielded from ambient thermal radiation in another experimental set up it read pressures lower than 1×10^{-15} Torr with appropriate corrections.

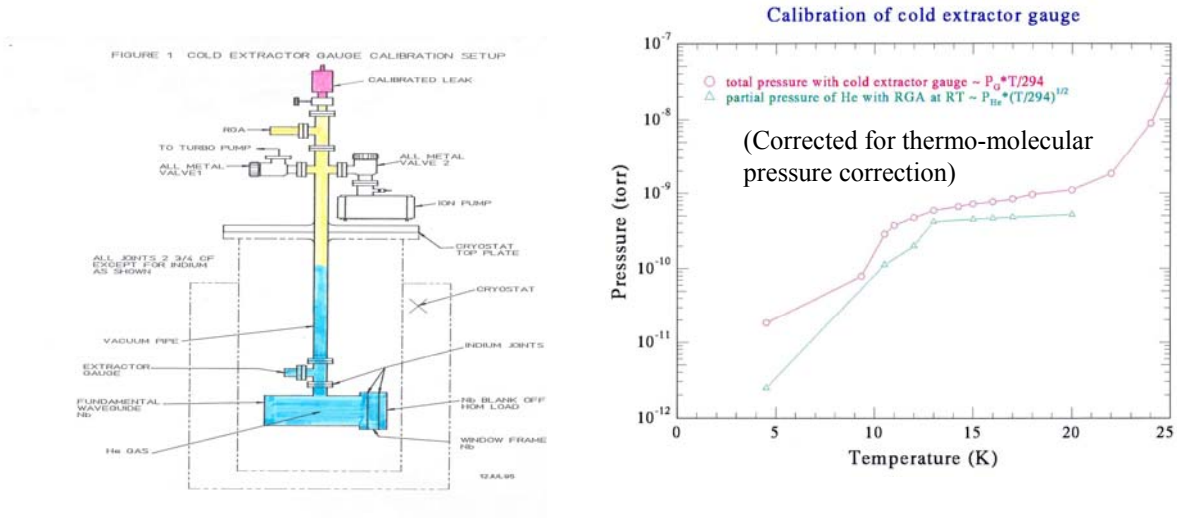

Figure 9: Cryogenic cross comparison between extractor gauge in a helium gas environment held at cryogenic temperatures and helium partial pressure measured by an RGA at room temperature. Ideal gas law governs relationship between pressures at different temperatures and can be used to determine sensitivity and minimum pressure readings achievable with an extractor gauge.

In Figure 10 the calibration setup of the extractor gauge with saturated vapor pressure of hydrogen is shown. The gauge under calibration is in the cryogen while the hydrogen leak valve, the RGA and another extractor gauge is at room temperature. The introduction of hydrogen into the vacuum chamber is controlled by the symetrical arrangement of holes in the feed tube, which extends all the way down into the vacuum chamber at liquid helium temperatures. This arrangement ensures that the hydrogen enters the vacuum system uniformly and covers the wall surfaces evenly and condenses to form mono to multi layers of hydrogen. After a monolayer of hydrogen is formed on the walls at 4.25 K, the pressure in the system increases exponential until it reaches its saturation vapor pressure of 1.39×10^{-6} Torr. The room temperature extractor gauge reads 1.48×10^{-6} Torr while the cold extractor gauge indicates 1.32×10^{-6} Torr. The cold gauge agrees quite well with the saturated vapor pressure and is with in the 5% measurement accuracy claimed by the manufacturer. The room temperature gauge reading is about 6.5% higher than the saturation vapor pressure of hydrogen since this reading may be affected by the local outgasing but it is quite good for all practical purposes. The difference in the initial gauge readings prior to the introduction of hydrogen gas can be attributed to the temperature difference, which indicates the higher outgassing rate (higher pressure) for the room temperature part of the vacuum system.

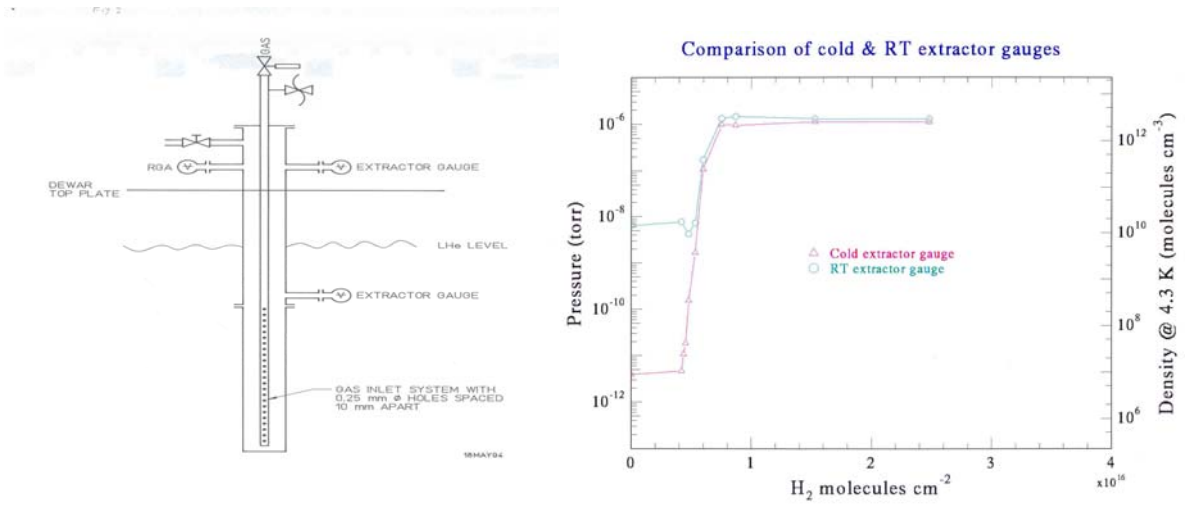

Figure 10: Similar cryogenic comparison using hydrogen vapour pressure measured by an extractor gauge at 4.25 Kelvin and hydrogen partial pressure measured by an extractor gauge and an RGA at room temperature. Data shows increasing adsorption of hydrogen on the walls from below a monolayer through saturation.

4. Barrier Coatings, Alternative Turbo Back Ups, Pump Limitations and Cryosorption Pumping

In this section we will discuss the effectiveness of barrier coatings on the outgassing rate of the vacuum chambers. We also report two alternative Turbo pump systems one backed by the conventional ion pump and the second one backed by the new active NEG pumps for improving the ultimate pressures and also to gain an understanding of the pumping mechanism limitations. In addition the use of metal sponges for generating XHV is also dealt with in detail.

4.1 Barrier Coatings

One method of achieving low outgassing rates for hydrogen is by applying simple and cost effective surface coating barriers. The lowering of the outgassing is conceived to be due to the reduction of the dissociation of water on the exterior surface of the stainless steel surface and the resultant minimization of dissociated H_2 interstitially permeating through the wall and recombining on the interior surface of the vacuum chamber.

A Pfeiffer TMU071P Turbo system backed by a MD4T diaphragm pump was used for evaluating the surface barrier coatings. Different treatments were applied to 304 stainless steel chambers with similar dimensions: silica coatings on both inner and outside walls with a thickness of ~1200 A^o (thicker silica coatings) and ~ 600 A^o (thinner silica coatings), silica coatings on outside only with a thickness of 1200 A^o (outside silica coating) and titanium oxide film of 1.2 μm coated only on the outside. The same procedure was adopted for the evaluation of all the chambers a) one day long initial evacuation before bake out after degreasing them in an ultrasonic bath and thoroughly rinsing them with ultra pure deionized water, b) baking at 180 ^{o}C for 24 hours and finally c) continually pumping and monitoring the vacuum for additional 24 hours.

Figure 11 summarizes the pumping curves for each of the four surfaces treated and one untreated stainless steel chambers. The chambers coated with the silica shows improvement in the pump down time as well as the ultimate pressure. Further tests for the optimum coating thickness and process may yield better results. Outgassing measurements indicate that there is a benefit over uncoated Stainless Steel.

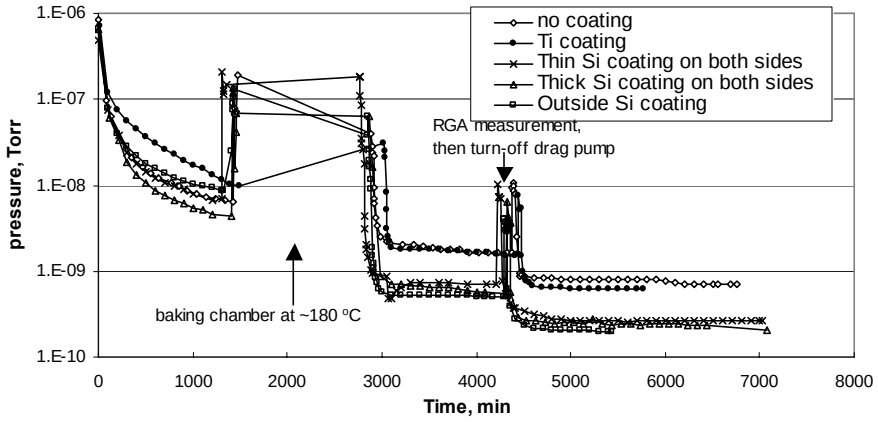

Figure 11: Pumpdown to ultimate pressure of several chambers: SS, Ti coated SS, and Silica coatings on SS. Pumping provided by turbo backed with scroll pump. Ultimate pressure of the three silica coated chambers is lower than the plain steel or Ti coated steel, indicating a reduction in outgassing rate assuming all other factors are equal.

4.2 Alternative Turbo Pump Backups

The first alternatively backed turbo was a Varian V70 LP with specifications as follows: pumping speed of 50 l/s, compression ratio for hydrogen of 7×10^4, and the base pressure achieved with the scroll as the backing pump was 1×10^{-9} Torr. The ion pump was a Varian Starcell 30 l/s, and was valved into the setup after it was started and allowed to run for several days. The foreline pressure of the turbo was maintained at 1×10^{-4} Torr which is an improvement over the scroll as a backing pump which kept the foreline of the turbo at 3 milliTorr. The ultimate pressure of the Turbo system was $1x10^{-10}$ Torr an order of magnitude lower. Helium backstreaming was eliminated and afforded a lower ultimate pressure.

This pumping system was used for comparing the performance characteristics of an AMF and silica coated stainless steel chambers [15]. The Japanese AMF chamber is made with Beryllium-Copper and is reported to have a very low outgassing rate (`<1×10-14 Torr l/scm^2) compared to silica-coated stainless steel. However they performed in a similar manner as shown in Figure 12 and this seems to be due to the ultimate pressure limitation of the Turbo pump system.

An active NEG cartridge from ALVATEC Corporation [3] was evaluated for its ability to pump on a foreline maintaining the turbo operation at the same level as a scroll-backing pump. The NEG pump was heated with a heat tape wrapped around the NEG and monitored for temperature to ensure that its seal opened. Figure 13 shows two trials at opening the seal. The heating current was increased to 5A, which finally made the seal open and the Scroll pump was valved out. The NEG can be seen to pump down the foreline to the same base pressure as the scroll and maintained this level for several days. Even if the NEG gets saturated it can be regenerated by further heating and this will bury the adsorbed gases there by providing fresh surface for further pumping.

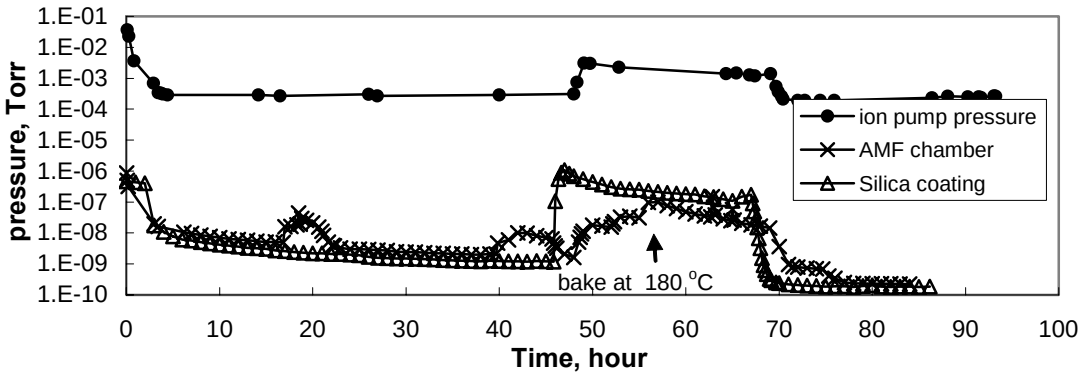

Figure 12: Ion pump backing a turbo pump through a bake. Ion pump is sufficient to handle gas load, but ultimate pressure achieved no better than with scroll pump in either the AMF chamber (a BeCu chamber manufactured by AMF) or Silica coated stainless steel chamber.

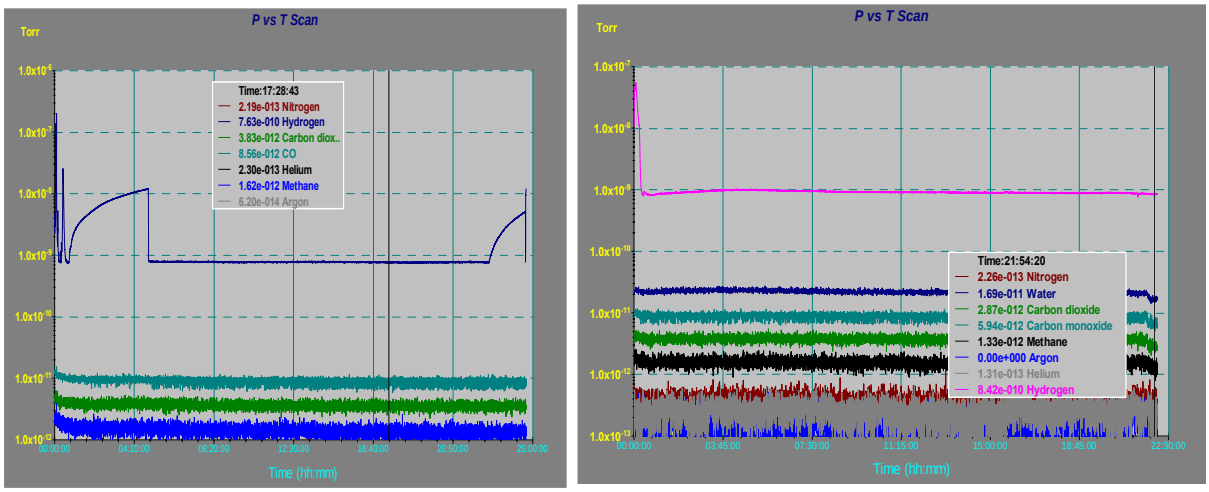

Figure 13: Two tries at unsealing active NEG pumps. The first shows pressure rise to an unstable level during two heating attempts. The second graph shows rapid pressure drop when the getter material is opened to the chamber and starts pumping.

4.2 Practical and Calculated Helium and Hydrogen Adsorption Isotherms for Various Surfaces

It is clear from the previous sections that the ultimate pressure of the vacuum system is basically limited by the performance characteristics of each of the pumping system. Cryosorption pumping of H_2 and He at temperatures 4.3 K and below is well known to reach ultimate pressures in the extreme high vacuum [16]. Figure 14 shows the practical adsorption isotherms of helium and hydrogen at 4.3 K for various technical surfaces as well as for the specially developed anodized aluminum. It can be seen that the adsorption capacity of aluminum oxide for hydrogen and helium is more than three orders of magnitude that of stainless steel, Al, Nb and niobium oxide.

Figure 15 presents the calculated adsorption isotherms of hydrogen based on the above measured isotherms, with the help of Dubinin and Radushkevich modified equation of Polyani potential theory of adsorption [16], for stainless steel and anodized aluminum. It is clear that hydrogen can be cryopumped to pressures in the extreme high vacuum range with anodized aluminum at 4.3 K with a large pumping capacity. It is also obvious that metal oxide sponges can easily be regenerated and they

provide particulate free XHV. Since no bonding agents are used there is unlikely to be a temperature difference between the pumping surface and the cooling system and hence the metal sponge is an ideal pumping system in the XHV range.

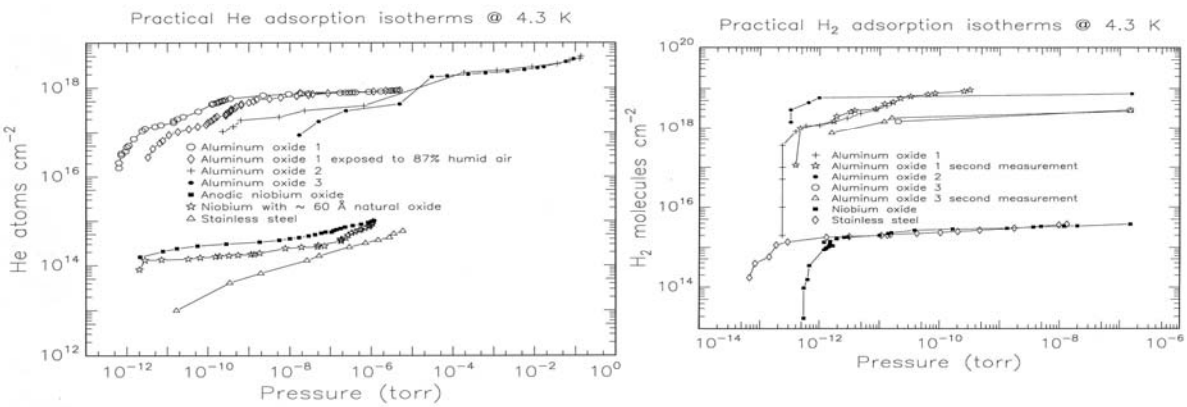

Figure 14: Measured helium and hydrogen adsorption isotherms. Data shows adsorption capacity of the three aluminium oxides at least two orders of magnitude higher than capacity of the niobium oxides and the bare stainless steel. For hydrogen, capacity of aluminium oxides is again greater than niobium oxide or bare stainless steel, though capacity drops rapidly at a critical base pressure of the system for hydrogen. [17]

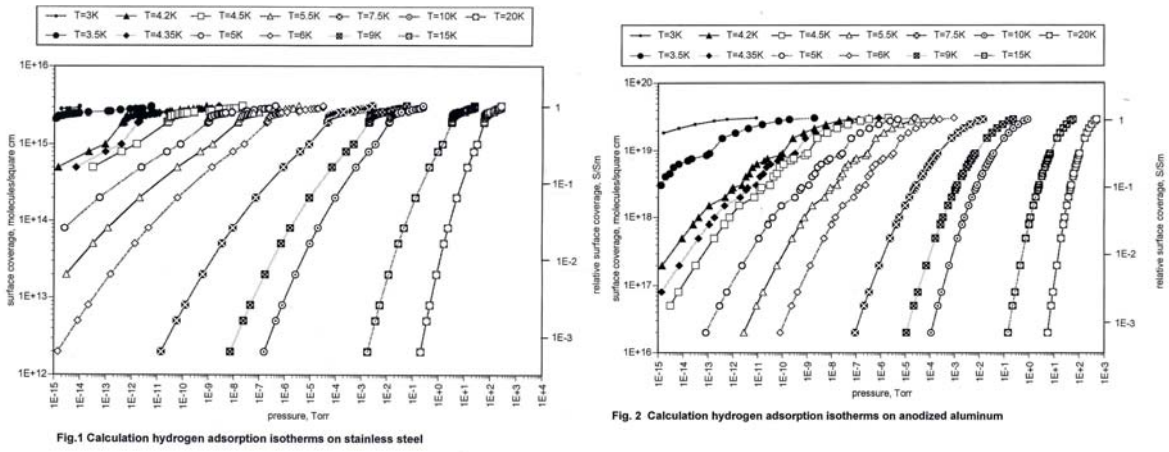

Figure 15: Calculated hydrogen adsorption isotherms on stainless steel and anodized aluminum.

5.0 Contamination control

The handling of all vacuum components and chambers require cleanroom quality gloves and lint free wipes. Other sources of contamination are due to airborne gases and particulates which must be controlled via flow hoods, complete filtration of purge and vent gasses, and nylon bags for transporting and storing parts. The use of Nano-filters for venting and purging has been shown to elliminate contaminents from systems used in superconducting technology applications where particulates are extremely problematic. Embracing these practices afford cleaner contaminant free systems and lower acheivable ultimate pressures.

The use of high-pressure de-ionized water rinses, as a final cleaning method has been shown to aid in the production of low ultimate pressures in vacuum systems and beamlines assembled for the Free Electron laser Facility (FEL) at Jefferson Lab [18]. Cleaning of vacuum components with Ozonated

water to remove hydro carbon species will eliminate recontamination of the system by the vacuum measuring instruments and this will afford improved results. An ozonated water facility is being setup to provide cleaner parts for our vacuum systems.

Discussion

Vacuum system characterization and improvements are useful in the quest for XHV. The major improvements include: gauge calibration for accurate pressure measurements, methods to characterize and quantify pumping from NEG coatings of chambers, an understanding of limitations of NEG pumps, characterizing the ion pump's pumping speed for methane and inert gasses which are not pumped by the NEGS, determining the ultimate pressure and limitations to ion pumps which limit the ultimate pressure of a NEG/ion pumped system, as well as implementing contamination controls. Further studies with Turbos and their backing pump methods promise better results which may provide additional pumping mechanisms for helping systems achieve lower pressures. The incorporation of a cyrosorption finger in the new load lock gun is likely to provide XHV by pumping methane and other oxides of carbon. Probably the simplest way of achieving XHV in the photoguns is to make the gun vacuum chamber with anodized aluminum and cool it to 4.2 K.

Acknowledgements

This work was supported by Jefferson Science Associates, LLC under U.S. DOE Contract No. DE-AC05-06OR23177. The authors would like to acknowledge the help of Jefferson Lab. Source & SRF Groups, C. Dong and P. Mehrotra.

References

[1] "Ultimate Pressure Limitations", J. *Vac. Sci*. Technol. **6**, 166 (1969) Bills, D.G.
[2] "Effect of Pretreatment on the Degassing of Materials", Trans. 8th AVS Vac. Symp. (Pergamon
[3] "New High Capacity Getter for Vacuum –insulated Mobile Liquid Hydrogen Storage Systems", Vacuum 82 (2008) 431-434 H. Londer, G. R. Myneni, P. Adderley, G. Bartlok, W. Knapp, D. Schleussner and E. Ogris
[4] "Evaluation of low cost RGA's for UHV applications" M. G. Rao and C. Dong, J. Vac. Sci. Technol. A 15(3) 1997 pp 1312-1318
[5] "High Vacuum Technology" A Practical Guide, 4.4, 95, Marsbed H. Hablanian, ISBN 0-8247- 99834-1
[6] "A Comparison of Outgassing Measurements for Three Vacuum Chamber Materials" M.L.Stutzman, P.Adderley, B.M.Poelker, M.Baylac, J. Clark, A.Day, J.Grames, J.Hansknecht, G.R.Myneni, P.M.Rutt and C.K.Sinclair in International Workshop on Hydrogen in Materials and Vacuum Systems , edited by G. Myneni and S. Chattopadhyay, AIP Conference Proceedings 671, Melville, New York, 2003, pp. 307-312
[7] "A novel approach to extreme vacua: the non-evaporable getter thin film coatings, C. Benvenuti, J. M. Cazeneuve, P. Chiggiatto, F. Cicoira, A. Escudeiro Santana, V. Johanek, V. Ruzinov, EST division, SM group, CERN, 1211 Geneva 23, Switzerland.
[8] "Characterization of the CEBAF 100 kV DC GaAs photoelectron gun vacuum system", Marcy Stutzman, Anthony Favale, Josh Brittian, James Clark, Joseph Grames, John Hansknecht, Ganapati Rao Myneni, Matt Poelker, Nuclear Instruments & Methods in Physics Research, Section A, Volume 574, 2007, page 213-220.
[9] "Measurements of photocathode operational lifetime at beam currents up to 10 mA using an improved DC high voltage GaAs photogun." J. Grames, M. Poelker, P. Adderley, J. Brittian, J. Clark, J. Hansknecht, D. Machie, M. L. Stutzman, K. Surles-Law, in Proceedings of the 17th International Spin Physics Symposium, kyoto Japan,ed. K Imai et al., 2006, p.1037
[10] "Processing Test Stand for the Fundamental Power couplers of the Spallation Neutron Source (SNS) Superconducting Cavities" M. Stirbet, I.E. Campisi, G.K. Davis, M. Drury, C. Grenoble, G. Myneni, T. Powers, K.M. Wilson (TJNAF) In proceedings of PAC 2001 p1143

[11] "Field Emitter Based Extractor Gauges and Residual Gas Analyzers" C. Dong and G. Rao Myneni J. Vac. Sci. Technol. A 17 (4) 1999 pp 2026-2033
[12] "Sensitive Helium Leak Detection in Cryogenic Vacuum Systems" M. G. Rao, Advances in Cryogenic Engineering Vol. 41 1996 pp 1783-1788
[13] "Recent Advances in UHV Techniques for Particle Accelerators" M. G. Rao In Proceedings of the IUVSTA95 Edited by N. Venkatesan and A. K. Sinha, 1995 pp 90-104
[14] "High Sensitivity helium Leak Detection Method" M. G. Rao J. Vac. Sci. Technol. A 11(4) 1993 pp 1598-1601
[15] "Methods for Reducing Hydrogen Outgassing" C. Dong, P. Mehrotra, and G. R. Myneni in International Workshop on Hydrogen in Materials and Vacuum Systems , edited by G. Myneni and S. Chattopadhyay, AIP Conference Proceedings 671, Melville, New York, 2003, pp. 307-312
[16] "The physical Basis of Ultra High Vacuum", P. A. Redhead, J. P. Hobson and E. V. Kornelsen American Institute of Physics 1993 P 46
[17] "Cryosorption Pumping of H2 and He with Metals and Metal Oxide at 4.3K M.G.Rao, P.Kneisel and J. Susta, Cryogenics, 34, 377-380 (1994).
[18] "Design and Installation of Low Particulate, Ultra-High Vacuum System for a High Power Free Electron Laser" H. F. Dylla, G. Biallas, L. Dillon-Townes, E. Feldl, G. R. Myneni, J. Parkinason, S. Willaims and M. Wiseman, J. Vac. Sci. Technol. A 17 (4) 1999 pp 2104-2108